

Contractile responses of engineered human μ myometrium to prostaglandins and inflammatory cytokines

Cite as: APL Bioeng. 8, 046115 (2024); doi: 10.1063/5.0233737

Submitted: 16 August 2024 · Accepted: 5 December 2024 ·

Published Online: 24 December 2024



View Online



Export Citation



CrossMark

Antonina P. Maxey,¹  Sage J. Wheeler,¹  Jaya M. Travis,¹  and Megan L. McCain^{1,2,a)} 

AFFILIATIONS

¹Laboratory for Living Systems Engineering, Alfred E. Mann Department of Biomedical Engineering, USC Viterbi School of Engineering, University of Southern California, Los Angeles, California, 90089, USA

²Department of Stem Cell Biology and Regenerative Medicine, Keck School of Medicine of USC, University of Southern California, Los Angeles, California, 90033, USA

Note: This paper is part of the Special Topic on Mechanomedicine.

^{a)}Author to whom correspondence should be addressed: mlmccain@usc.edu

ABSTRACT

Preterm labor is a prevalent public health problem and occurs when the myometrium, the smooth muscle layer of the uterus, begins contracting before the fetus reaches full term. Abnormal contractions of the myometrium also underlie painful menstrual cramps, known as dysmenorrhea. Both disorders have been associated with increased production of prostaglandins and cytokines, yet the functional impacts of inflammatory mediators on the contractility of human myometrium have not been fully established, in part due to a lack of effective model systems. To address this, we engineered human myometrial microtissues (μ myometrium) on compliant hydrogels designed for traction force microscopy. We then measured μ myometrium contractility in response to a panel of compounds with known contractile effects and inflammatory mediators. We observed that prostaglandin F_{2 α} , interleukin 6, and interleukin 8 induced contraction, while prostaglandin E1 and prostaglandin E2 induced relaxation. Our data suggest that inflammation may be a key factor modulating uterine contractility in conditions including, but not limited to, preterm labor or dysmenorrhea. More broadly, our μ myometrium model can be used to systematically identify the functional impact of many small molecules on human myometrium.

© 2024 Author(s). All article content, except where otherwise noted, is licensed under a Creative Commons Attribution-NonCommercial 4.0 International (CC BY-NC) license (<https://creativecommons.org/licenses/by-nc/4.0/>). <https://doi.org/10.1063/5.0233737>

INTRODUCTION

Approximately one of every eight infants in the United States is born premature, which is the leading cause of neonatal death.¹ The incidence of premature birth is high in large part because treatment options for spontaneous preterm labor, the most common precursor to premature birth, are extremely limited. For example, a synthetic analog of progesterone is commonly administered as a preventative treatment for patients at risk of spontaneous preterm labor, but is only effective in one-third of recurrent preterm births.² Once preterm labor has begun, some drugs, such as the β_2 adrenergic receptor agonists terbutaline and ritodrine, can temporarily delay labor, but rarely to never prevent preterm birth.³

Spontaneous preterm labor occurs when the smooth muscle layer of the uterus, known as the myometrium, initiates contractions before the fetus reaches full term.^{4,5} Abnormal myometrial contractions also underlie dysmenorrhea in non-pregnant patients, a condition that

affects at least 45% of childbearing-aged females and is characterized by painful menstrual cramps.^{6,7} Interestingly, patients who experience dysmenorrhea pre-conception are at higher risk of experiencing preterm labor when pregnant,^{8,9} suggestive of overlapping etiology of these two conditions. Therefore, establishing the underlying and potentially convergent causes of dysmenorrhea and preterm birth could lead to more successful treatments for these and other disorders caused by abnormal myometrial contractions.

Dysmenorrhea and spontaneous preterm labor are also both associated with increased presence of inflammatory prostaglandins and cytokines.^{10,11} Prostaglandins are bioactive lipids with hormone-like effects that are produced by many tissues, including the endometrium,¹² fetal membranes,^{13,14} and placenta.¹³ Increased production of prostaglandins is considered as one of the primary events preceding preterm labor.¹⁵ Elevated prostaglandins are also observed in patients with dysmenorrhea,¹⁶ which is commonly treated by reducing

prostaglandin production with non-steroid anti-inflammatory drugs (NSAIDs),¹⁷ although these have a failure rate of approximately 20%–25%.⁶ Increased levels of cytokines have also been observed in the serum¹⁸ and plasma¹⁹ of patients who deliver preterm and in the plasma of patients with dysmenorrhea.²⁰ Cytokines are secreted by many cell types, including the endometrium,^{21,22} and primarily regulate immune cells. However, select cytokines can also induce hypercontractility in airway smooth muscle.^{23–25} Similarly, prostaglandins have been shown to modulate the contraction of bladder smooth muscle²⁶ and vascular smooth muscle.²⁷ Studies with uterine tissue explants have shown that distinct types of prostaglandins induce myometrial contraction or relaxation, depending on the prostaglandin receptor subtype.^{28–30} Cytokines have also been shown to stimulate myometrial contractions in explanted rabbit uterine tissue,³¹ which, according to an *in vitro* study with human cells, may be due to the stimulation of oxytocin production.³² These studies motivate more investigation into the effects of inflammatory mediators on myometrial contractility, especially given the vast number of prostaglandins, cytokines, receptor subtypes, and cell types involved in processes such as spontaneous preterm labor. These studies also urge the development of new model systems that can be used to systematically evaluate the direct impact of small molecules on the contractility of human myometrium, as existing model systems have many limitations.³³ For example, human uterine tissue strips are difficult to acquire, have very limited survival in culture, and have low reproducibility due to many confounding factors, such as patient-to-patient variability and heterogeneous cellular composition.³⁴ Animal models are also limited due to the many fundamental differences in pregnancy and parturition between species.³⁵

Traction force microscopy (TFM) is a technique that has been widely used to quantify contractile forces generated by many cell types, including epithelial cells,³⁶ cardiomyocytes,³⁷ and airway smooth muscle cells.³⁸ TFM is performed by culturing cells on a hydrogel (or other compliant surface) doped with fluorescent microbeads, which are tracked as the cells generate force and deform the hydrogel.³⁹ We and others have improved the reproducibility of TFM measurements by micropatterning shape-controlled cells and tissues on the surface, which localizes focal adhesion attachments (and thus force transmission) to relatively consistent locations.^{40–42} In this study, we engineered human myometrial microtissues, which we call μ myometrium, and implemented TFM to evaluate their contractile response to contractile agonists, antagonists, and inflammatory mediators. Our results show that oxytocin, prostaglandin F₂-alpha (PGF), interleukin 6 (IL-6), and interleukin 8 (IL-8) induced contraction of μ myometrium while prostaglandin E₁ (PGE₁) and prostaglandin E₂ (PGE₂) induced relaxation. These data suggest that human myometrium has a direct contractile response to inflammatory mediators, which may play a role in spontaneous preterm labor or other conditions associated with both inflammation and abnormal myometrial contractility, such as dysmenorrhea. More broadly, the μ myometrium assay that we established here can be broadly used to evaluate human myometrial contractility in response to many compounds and help develop more effective therapies for patients experiencing uterine disorders.

RESULTS

Engineering human μ myometrium

As described above, spontaneous preterm labor and dysmenorrhea are two examples of disorders associated with abnormal

myometrial contractions that are difficult to investigate due to a lack of human-relevant model systems with functional readouts. To address this, we first engineered myometrial microtissues (μ myometrium) by culturing primary human myometrial cells on an array of fibronectin rectangles ($200 \times 100 \mu\text{m}^2$) microcontact printed on polyacrylamide hydrogels bonded on glass coverslips [Fig. 1(a)], similar to approaches previously developed for cardiomyocytes.^{40–42} As expected, the cells adhered to the fibronectin rectangles, forming arrays of shape-controlled aligned μ myometrium with minimal cell adhesion outside of the fibronectin pattern [Fig. 1(b)]. Myometrial smooth muscle cells similarly align into anisotropic tissues *in vivo*.⁴⁴ We then stained coverslips for fibronectin, DAPI, and actin to evaluate tissue structure ($n = 25$ tissues). Based on fibronectin immunostaining, tissues had an average length of $215.2 \pm 2.3 \mu\text{m}$, width of $109.5 \pm 1.7 \mu\text{m}$, and aspect ratio of 1.98 ± 0.02 [Fig. 1(c)], indicating that tissue size was relatively consistent. We also found that the average number of nuclei per tissue was 37 ± 2.5 and ranged between 21 and 62, likely due to slight variation in cell seeding and attachment [Fig. 1(c)]. Finally, we quantified the orientation of actin filaments. As expected, the rectangular shape of the fibronectin micropattern induced actin filaments to align uniaxially [Fig. 1(d)], similar to native myometrium.

Contractile response to oxytocin

Oxytocin is a naturally occurring hormone that induces myometrial contractions and its synthetic analog is the most commonly used drug to induce labor.⁴⁵ Thus, we next measured basal and oxytocin-induced forces generated by engineered μ myometrium. We followed the same fabrication steps described above (Fig. 1), with the addition of fluorescent microbeads in the polyacrylamide hydrogels. We then transferred each coverslip to an inverted fluorescence microscope, positioned a single μ myometrium in the field of view, and captured a phase contrast image of the tissue and an image of the embedded fluorescent beads [Fig. 2(a)]. Next, we added synthetic oxytocin (0.5 mM) and captured images each minute for 12 min [Fig. 2(b)]. Finally, we added trypsin to detach cells and continued imaging each minute for six additional minutes [Fig. 2(c)]. Based on the images of the fluorescent beads and the elastic modulus of the hydrogel (1 kPa), we calculated the displacement, stress, and force generated by each tissue at each timepoint relative to its starting timepoint. As shown in Fig. 2(d) and SI Video 1, engineered μ myometrium responded as expected by generating force in response to oxytocin, which plateaued after about 5 min. In response to trypsin, the tissue detached completely from the hydrogel and the beads displaced beyond their initial location, confirming that these smooth muscle cells exerted a basal force on the substrate, as expected. We also observed that force transmission was concentrated at the longitudinal ends of the tissue, similar to previous studies with engineered cardiac myocyte microtissues.^{43,46} We expect that, similar to cardiac myocytes, myometrial smooth muscle cells are detaching cell–matrix adhesions in the center of the tissue in favor of cell–cell adhesions and thus function more like a syncytium.

Next, we statistically compared induced forces generated by μ myometrium in response to PBS vehicle or 0.5 mM oxytocin. As shown by the representative images in Fig. 3(a), displacement and traction stress increased when oxytocin was added compared to PBS. When comparing multiple tissues, the amount of force generated by μ tissues treated with oxytocin was significantly higher than the PBS vehicle control [Fig. 3(b)]. The amount of basal force generated by

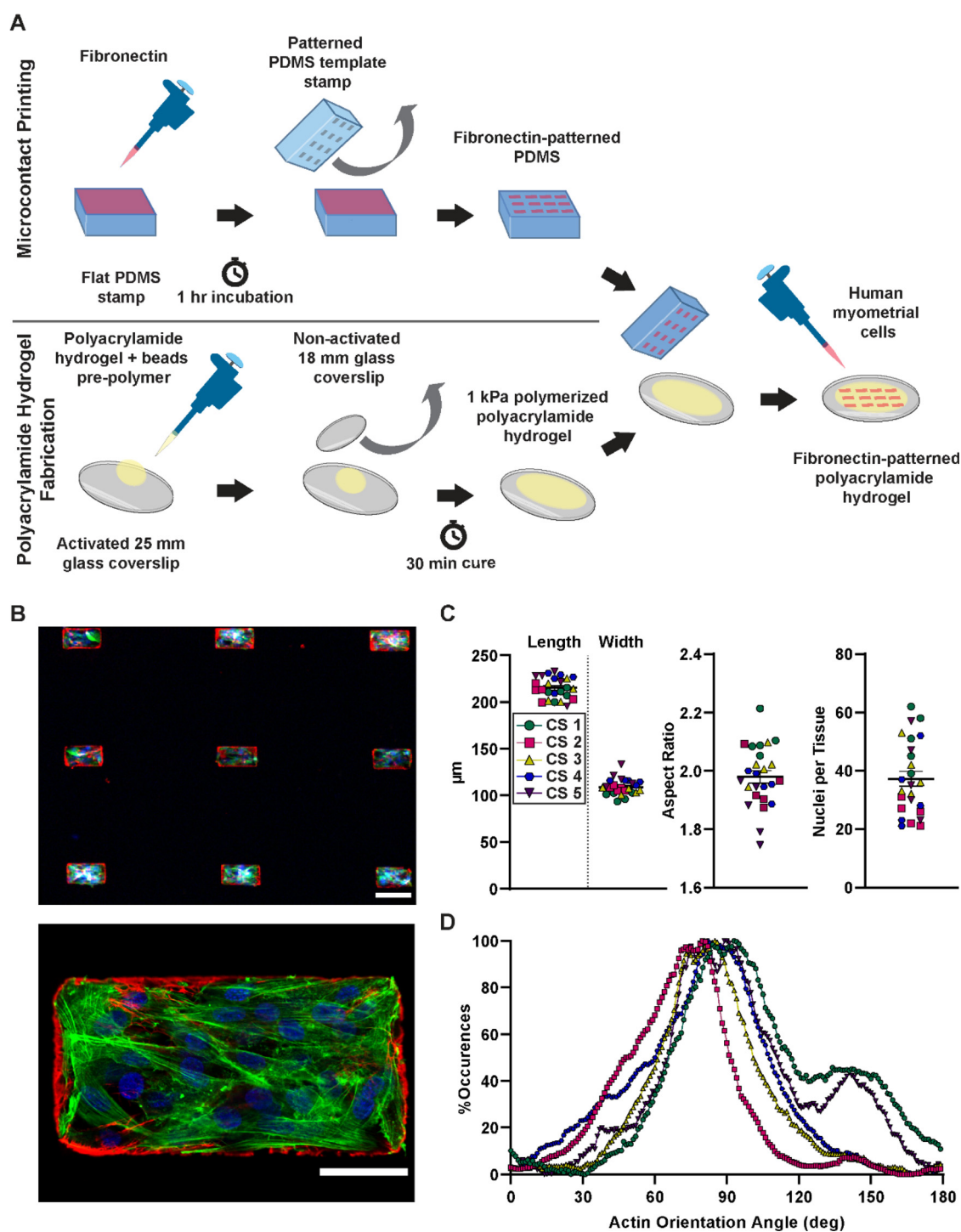


FIG. 1. Engineering and characterizing human μ myometrium. (a) Polyacrylamide hydrogels were fabricated on glass coverslips, micropatterned with an array of fibronectin rectangles, and seeded with primary human myometrial cells to engineer $200 \times 100 \mu\text{m}^2$ human myometrial microtissues (μ myometrium). (b) Human μ myometrium stained for fibronectin (red), nuclei (blue), and f-actin (green). Scale bars: $200 \mu\text{m}$ (top) and $50 \mu\text{m}$ (bottom). (c) Length, width, and aspect ratio of micropatterned fibronectin rectangles (mean \pm standard error of the mean, $n = 25$ tissues) distributed amongst five coverslips (CS). Each CS is indicated by a different color and shape. (d) Histogram of actin orientation angles averaged across five μ myometrium per CS. Each CS is indicated by a different color and shape.

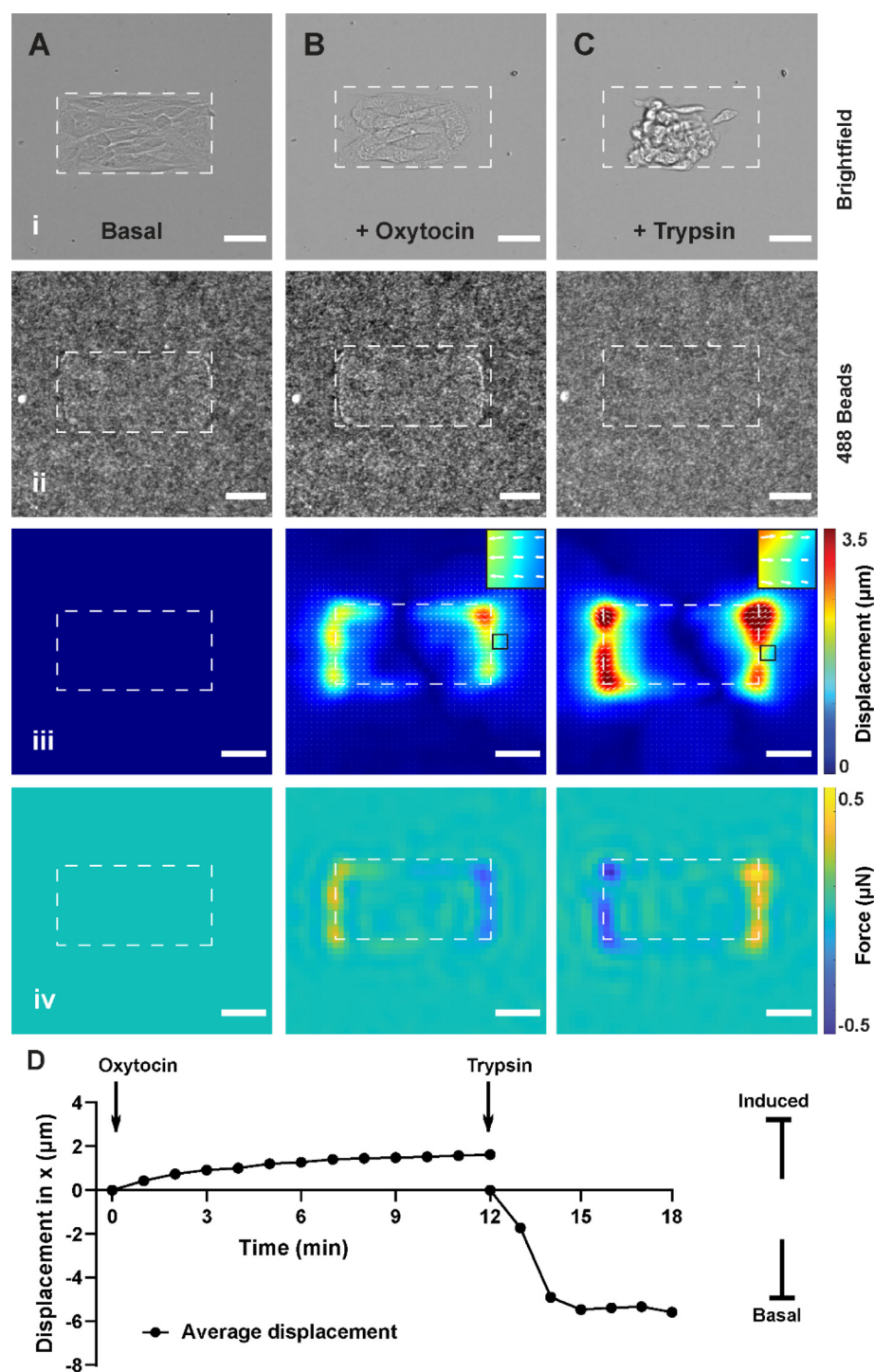


FIG. 2. Measuring basal and oxytocin-induced contractile responses of μ myometrium. (a) Tissues at baseline exert basal tension on the polyacrylamide hydrogel, as shown in the brightfield (i) and fluorescent bead image (ii). Displacement map (iii) and force map (iv) are null because this is the reference timepoint. (b) Oxytocin induces contraction, as shown by brightfield (i) and bead images (ii), displacement vectors pointing inward (iii), and inward force map (iv). (c) Trypsin removes cells (i), resulting in outward bead movement (ii), displacement (iii), and force (iv). Scale bars: $50\ \mu\text{m}$. (d) Displacement over time for a representative sample. Each dot represents an average of the three maximum displacement vectors at that time point. Positive values indicate contraction and negative values indicate relaxation or release of tension.

tissues (before addition of oxytocin or PBS) was not statistically significant [Fig. 3(b)], but did show some variation, likely due to slight differences in fibronectin patterning, cell seeding, etc. Thus, μ myometrium contracted in response to acute stimulation with oxytocin, as expected.

Response to contractile antagonists

We next asked if μ myometrium would respond to contractile antagonists. Thus, we pretreated μ myometrium with progesterone or caffeine, which are each expected to elicit a weaker contractile

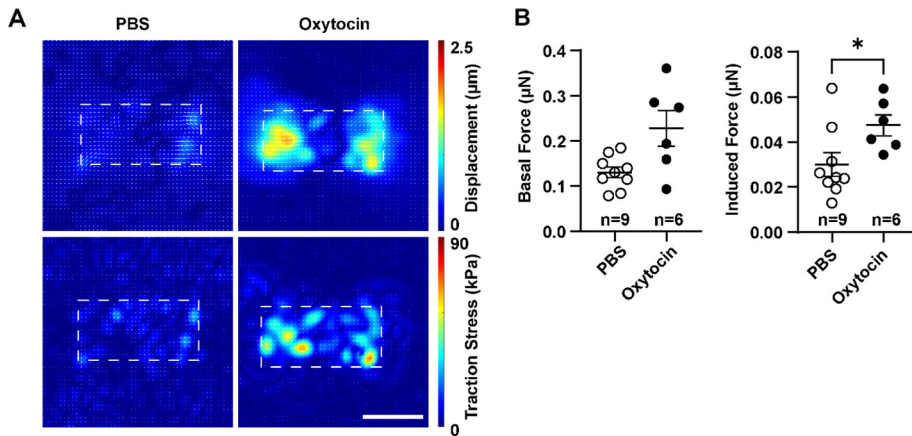


FIG. 3. Displacement and traction stress in response to oxytocin stimulation. (a) Representative displacement (top row) and traction stress (bottom row) maps at the peak frame of contraction induced by PBS or 0.5 mM oxytocin in PBS. Dashed white boxes approximate the tissue borders before oxytocin is added. Scale bar: 100 μm . (b) Quantification of basal and induced forces exerted by $\mu\text{myometrium}$ (mean \pm standard error of the mean). * denotes $p < 0.05$ using unpaired t-test.

response. Progesterone is an endogenous hormone that maintains the myometrium in a quiescent state.⁴⁷ Natural progesterone and its synthetic analogs are used clinically to mitigate preterm labor.⁴⁸ When we pretreated tissues with progesterone for at least 12 h, the basal force

trended lower but did not reach statistical significance [Figs. 4(a)–4(c)]. Induced force in response to oxytocin in tissues pretreated with progesterone was unchanged. We also tested the effects of 10 min of pretreatment with caffeine, a compound that is commonly

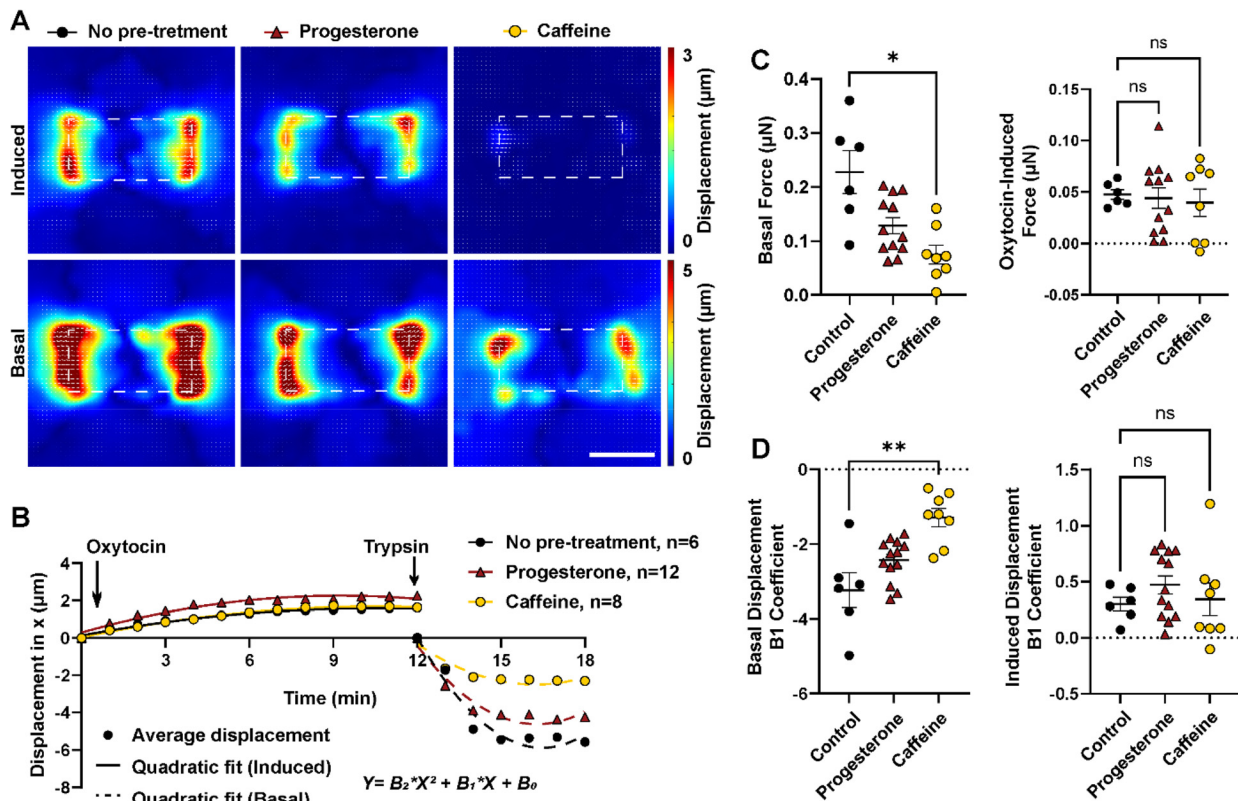


FIG. 4. Responses to contractile antagonists. (a) Representative peak displacement maps for $\mu\text{myometrium}$ pretreated with indicated contractile antagonist and acutely treated with oxytocin to measure induced force (top row), followed by trypsinization to measure basal force (bottom row). Dashed white boxes approximate the tissue borders before oxytocin is added. (b) Average displacement vs time for $\mu\text{myometrium}$ with no pretreatment ($n = 6$), pretreatment with progesterone ($n = 12$), or pretreatment with caffeine ($n = 8$) and then acutely treated with oxytocin followed by trypsin. Second order polynomial curves were fit to the oxytocin-induced displacement data (solid line) and basal displacement data (dashed line). (c) Basal and oxytocin-induced forces at maximum displacement. (d) Second coefficient (B_1) of second order polynomial fit for basal and induced displacement curves. * denotes $p < 0.05$, ** denotes $p < 0.01$ using Dunnett’s multiple comparisons test. Scale bar: 100 μm .

contra-indicated during pregnancy. Caffeine pretreatment with a concentration similar to that used in other smooth muscle models^{49,50} significantly reduced the basal force but did not impact oxytocin-induced force, aligning with our previous findings that caffeine decreases calcium transient duration in these cells.⁵¹ Rodent studies have also shown that caffeine induces relaxation of uterine smooth muscle cells.^{52,53} Thus, both progesterone and caffeine had a greater impact on basal force compared to oxytocin-induced force.

In addition to evaluating force values at peak displacement, we fit a second order polynomial curve to the displacement vs time data after oxytocin addition (induced) to better evaluate the full range of displacement data for each sample. We also fit another second order polynomial curve to the displacement vs time data after trypsin addition (basal). We then compared the second coefficient (B1) of the fit curves because this parameter reflects the tilt and horizontal stretch of the parabola. The B1 parameter showed similar trends to the force data [Fig. 4(d)], indicating that this is also a useful metric of μ myometrium function that accounts for all data points in the timecourse.

Contractile response to inflammatory mediators

We next tested the acute impact of prostaglandins, hormone-like molecules that fluctuate through pregnancy and menstruation, on μ myometrium contraction. For these experiments, cells were not pretreated with any compounds, and prostaglandins were used in place of oxytocin to acutely stimulate contractile responses. PGF, a prostaglandin that has been shown to induce contractions *in vitro* in pregnant and non-pregnant tissue,⁵⁴ caused tissues to contract [Figs. 5(a)–5(c)].

Prostaglandin E1 (PGE1) is used clinically in the form of misoprostol to induce uterine contractions.⁵⁵ As such, we expected to see the tissues contract in response to a bolus of PGE1, but instead observed relaxation [Figs. 5(a)–5(c)], which may be attributed to regional differences in prostaglandin receptors across the uterus.⁵⁶ Similarly, we observed relaxation in response to PGE2 [Figs. 5(a)–5(c)]. We observed similar basal forces for all conditions, as expected [Figs. 5(a)–5(c)]. The second coefficient B1 of a second order polynomial fit to the induced and basal displacement data showed similar trends as the force data [Figs. 5(c) and 5(d)]. Thus, our assay enabled us to distinguish between the contractile or relaxant effects of specific prostaglandins.

Finally, we tested the acute effects of interleukins IL-6 and IL-8 on contraction of μ myometrium. Both IL-6 and IL-8 caused tissues to contract and exhibit a statistically significant increase in force compared to the PBS vehicle control [Figs. 6(a)–6(c)]. This is contrary to the lack of contraction observed in a rat myometrium model,⁵⁷ which may be due to species-specific differences. Prior to cytokine treatment, all tissues exhibited similar basal force [Fig. 6(c)] as expected since tissues were not pretreated. Similar to the previous datasets, the second coefficient B1 of a second order polynomial function fit to the displacement data reflected similar trends as the force data [Figs. 6(c) and 6(d)]. Thus, engineered human μ myometrium contracted in response to acute IL-6 and IL-8 stimulation.

DISCUSSION

Due to the lack of human models to investigate disorders associated with dysfunctional uterine contractility, such as spontaneous preterm labor, we engineered human μ myometrium and validated their

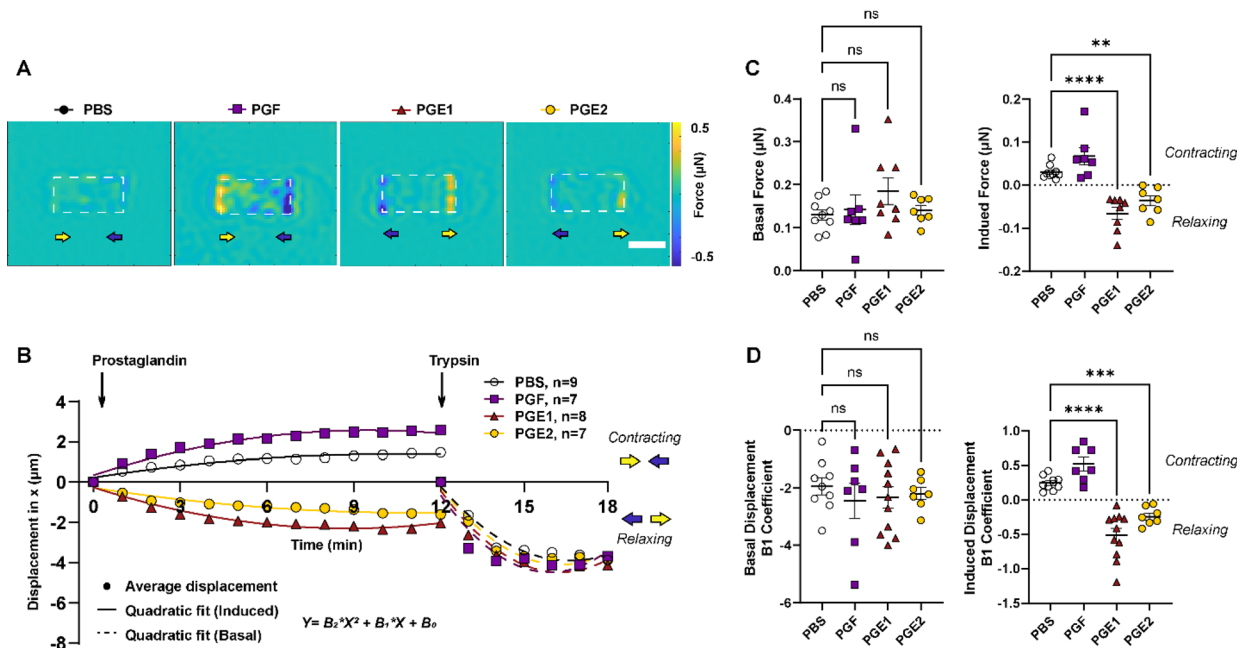


FIG. 5. Contractile responses to prostaglandins. (a) Representative force maps with arrows indicating the direction of bead movement in response to each prostaglandin (PG) or PBS vehicle control. Dashed white boxes outline the tissue borders before PG is added. Scale bar: 100 μ m (b) Average displacement vs time after the acute addition of vehicle (phosphate buffered saline, PBS) ($n = 9$), PGF ($n = 7$), PGE1 ($n = 8$), and PGE2 ($n = 7$), then trypsin. Second order polynomial curves were fit to the induced displacement data (solid line) and basal displacement data (dashed line). (c) Basal and induced forces at maximum displacement. (d) Second coefficient (B1) of second order polynomial fit for basal and induced displacement curves. ** denotes $p < 0.01$, *** $p < 0.001$, and **** $p < 0.0001$, using Dunnett's multiple comparisons test.

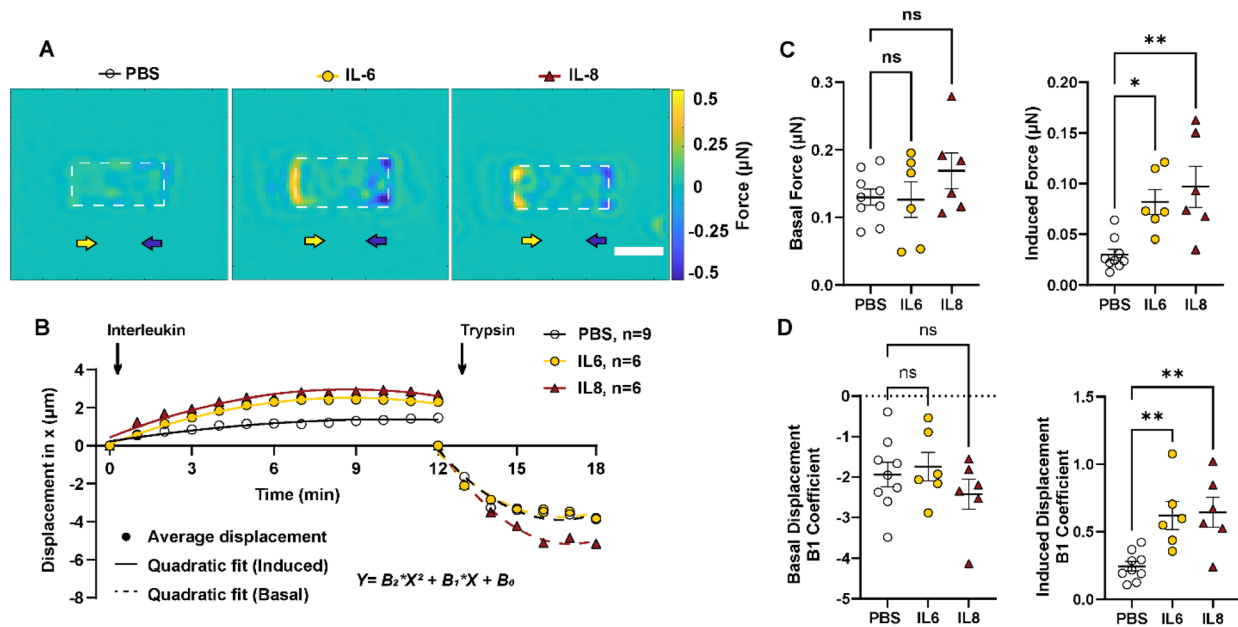


FIG. 6. Contractile responses to interleukins. (a) Representative force plots with arrows indicating the direction of bead movement in response to each interleukin (IL) or PBS vehicle control. Dashed white boxes outline the tissue borders before IL is added. Scale bar: 100 μm . (b) Average displacement vs time after the acute addition of vehicle (phosphate buffered saline, PBS) ($n = 9$), IL-6 ($n = 6$), and IL-8 ($n = 6$), then trypsin. Second order polynomial curves were fit to the induced displacement data (solid line) and basal displacement data (dashed line). (c) Basal and induced forces at maximum displacement. (d) Second coefficient (B1) of second order polynomial fit for basal and induced displacement curves. * denotes $p < 0.05$ and ** $p < 0.01$, using Dunnett's multiple comparisons test.

contractile response to known contractile agonists and antagonists using a traction force microscopy assay. We found that $\mu\text{myometrium}$ contracted in response to oxytocin and relaxed in response to caffeine, as expected. We then probed the effects of inflammatory mediators on our engineered tissue model and observed contraction in response to PGF, IL-6, and IL-8 and relaxation in response to PGE1 and PGE2. Together, these data indicate novel links between inflammation and uterine contractility and illustrate how our model can be used to systematically investigate the contractile response of human myometrium to small molecules.

We first challenged our $\mu\text{myometrium}$ model with oxytocin, a hormone naturally produced primarily by the hypothalamus⁵⁸ during labor to stimulate uterine contractions. During spontaneous labor, pulses of oxytocin gradually increase in frequency and amplitude as labor progresses. Patient blood samples indicate that oxytocin is present at approximately 20 pM during early labor and up to 200 pM during late stages of labor, although measurements are highly variable.^{59,60} Synthetic oxytocin is also the most commonly used drug to induce labor under the brand name Pitocin,⁴⁵ which is typically administered at 2–16 mU/min (3.3–26.7 pg/min).⁶⁰ In this study, we used 0.5 mM oxytocin, which is much higher than the concentrations measured in pregnant patient blood.⁵⁹ However, neighboring reproductive tissues, such as the decidua, also produce oxytocin,^{58,61} which may create a higher local concentration within the tissue compared to circulating blood. We also do not know the pregnancy state of the patient who donated the cells used for our study, which is relevant because oxytocin receptor expression is lowest in non-pregnant myometrium and highest in pregnant myometrium at term.⁶² Furthermore, we expect that all cells lose some expression of oxytocin receptors during *in vitro* culture

and thus become less sensitive to oxytocin. Despite these caveats, we found that oxytocin induced contractions with significance compared to the vehicle control, which can likely be attributed to increased binding to oxytocin receptors that resulted in a greater sensitivity to calcium and a larger influx of intracellular calcium.⁶³ These results show that our tissues retained contractile function and measurable oxytocin sensitivity *in vitro*, and also align with our previous findings that calcium fluorescence amplitude in human myometrial smooth muscle cells increases in response to oxytocin.⁵¹

Next, we tested if contractile antagonists would suppress contractions. Progesterone is a steroid hormone synthesized primarily by the corpus luteum in non-pregnant patients and primarily by the placenta in pregnant patients. Progesterone maintains myometrial quiescence and thus is required for pregnancy maintenance.⁶⁴ We found that tissues incubated for at least 12 h in progesterone exhibited a slightly lower basal force, yet minimal change to oxytocin-induced force. One explanation for this trend may be that progesterone has both genomic and non-genomic effects that function on different time scales. For example, the decrease in basal force could be caused by a non-genomic mechanism, such as inhibition of G-protein coupled signal transduction, that takes effect more quickly. The genomic effects of progesterone, such as inhibiting translation of the oxytocin receptor gene, may need more time to develop and impact oxytocin-induced contractions.⁶⁵ This trend aligns with the clinical use of progesterone as a long-term preventative treatment instead of an acute treatment.⁶⁶ Cells likely also lose some sensitivity to progesterone during *in vitro* culture, which we attempted to offset, at least in part, by using concentrations of progesterone in our study (0.127 mM) much higher than those measured in the serum of pregnant women (>10 ng/ml or >32 nM).^{67,68}

Of note, exogenous progesterone is applied at relatively high concentrations to try to quell spontaneous preterm birth, such as 200 mg (0.6 mmol) three times a day.⁶⁸ Caffeine-treated tissues also exhibited significantly reduced basal forces. Caffeine has consistently been shown to relax smooth muscle,^{49,52} but is also discouraged during pregnancy due to its association with preterm labor.⁶⁹ However, associations between caffeine and preterm labor have been attributed to caffeine-induced increases in fetal heart rate and movement,⁷⁰ not increased myometrial contractility, which is consistent with our findings. These examples highlight that our platform can help dissect the direct effects of compounds on both the basal and induced contractility of human myometrium, independent from other pregnancy-related cells and tissues that may introduce confounding variables.

Many reproductive tissues, including endometrial cells, produce arachidonic acid, which is converted by cyclooxygenase into prostaglandins.^{71,72} Patients with dysmenorrhea exhibit elevated plasma prostaglandin concentrations, ranging from 32 to 105 pg/ml, compared to the 20–22 pg/ml observed in patients without dysmenorrhea.¹⁶ NSAIDs are commonly prescribed to patients with dysmenorrhea because they reduce prostaglandin production by inhibiting cyclooxygenase.¹² *In vitro* experiments with non-human myometrial cells have shown that prostaglandins can lead to contraction or relaxation, depending on the prostaglandin subtype and binding receptor.⁷³ The prevalence of receptor types also varies regionally in the uterus, as the lower uterus usually needs to be more relaxed than the upper uterus such that the fetus can be delivered.^{74,75} With our platform, we tested the effects of individual prostaglandins. We found that PGE1 caused μ myometrium to relax, which contrasts with its clinical use in inducing labor.⁷⁶ However, our myometrial cells were obtained from a company that does not report the region of origin within the uterus. Thus, it is possible that these cells were retrieved from the lower uterus or are a mixture of cells sourced from multiple regions of the uterus. PGE1 is also known to impact labor by mechanisms that are independent of the myometrium, such as reducing collagen cross-linking in the cervix,²⁹ and these effects would not be captured in our model. In non-pregnant tissue, PGE2 has been shown to exhibit both contractile and relaxant behavior due to different receptor subtypes, which may explain why it caused relatively minor relaxation in our study and others.^{77,78} Future work could account for the region of origin during cell isolation from the uterus such that region-dependent differences in prostaglandin receptors could be identified.

Interleukin levels fluctuate throughout a normal menstrual cycle and pregnancy. Interleukin levels generally peak at times of heightened contractility, including the early follicular phase of the menstrual cycle, when the endometrium is sloughed off, and during the last trimester of pregnancy, when the fetus is pushed out. Serum levels of interleukins IL-6 and IL-8 are also increased in patients who experience dysmenorrhea and preterm labor.^{18–20} For example, one study observed that IL-6 levels in cervical fluid were significantly elevated in patients experiencing preterm labor, with a concentration of approximately 600 pg/L compared to just 60 pg/L in patients experiencing term labor.⁷⁹ Thus, excessively high levels of interleukins may contribute to abnormal contractile behavior during menstruation and/or pregnancy. Our observation that IL-6 and IL-8 stimulated contractions of engineered myometrium supports the theory that interleukins impact the contractile behavior of the uterus. Given this potential causative relationship, IL-6 and IL-8 may be considered as predictive biomarkers of

contractile pathologies, and establishing more robust reference intervals may aid clinicians in providing more effective treatments. In addition, interleukins or their receptors may be promising targets for therapeutic intervention. For example, Tocilizumab is an IL-6 receptor inhibitor that has been approved for treatment of rheumatoid arthritis⁸⁰ and may also be considered as a treatment of uterine contractile disorders.

As with oxytocin and progesterone, an important caveat for our experiments with prostaglandins and interleukins is that our *in vitro* concentrations greatly exceeded the measured concentrations in patient fluid samples. However, also similar to oxytocin, we cannot clearly measure or predict the local concentration of these factors within the myometrium, and we expect cells *in vitro* to lose some sensitivity to these molecules. Furthermore, in this study, we focused on the acute contractile effects of these factors. However, long-term exposure to these inflammatory factors likely occurs *in vivo* and may cause remodeling of the cells at the transcriptional level. Thus, evaluating both contractility and cell remodeling after longer incubations with these factors is an important topic for follow-up studies.

Our model is a highly simplified system that is advantageous for systematically measuring the direct impact of small molecules on the contractility of human myometrium without other confounding factors. Due to its simplicity, our model is also relatively easy to scale-up for medium-throughput applications. However, our model is lacking any form of vascularization, which is an important source of paracrine signaling factors and also controls the delivery of drugs and other small molecules from the blood to myometrial smooth muscle cells. The vasculature in the myometrium also undergoes extensive remodeling during pregnancy.⁴⁴ Thus, vascularization is an important feature to consider for future iterations of our model, especially to improve its suitability for applications in drug screening. Many immune cells are also embedded in human myometrium,⁸¹ which are key regulators of cytokine signaling and should also be integrated in future models of the myometrium, similar to recent work in engineered cardiac tissue models.⁸² We also anticipate that 3-D engineered myometrium models,⁸³ which can also be selectively doped with supporting cell types, may demonstrate enhanced maturity and sensitivity to small molecules, as observed in other engineered muscle systems.^{84,85} Other tissues in the female reproductive system, such as the placenta, fetal membrane, and decidua, also produce and are impacted by cytokines^{86–88} and prostaglandins.¹³ Thus, our model could be further advanced by pairing it via microfluidics to other engineered models of female reproductive tissues, such as the endometrium,^{89,90} placenta,^{91,92} or EVATAR, a multi-compartment microfluidic system with ovary, fallopian tube, cervix, liver, and endometrium.⁹³

Collectively, due to the many cell and tissue types present in the female reproductive system, models that can systematically incorporate crosstalk between distinct cell and tissue types and provide quantitative functional readouts will be invaluable for establishing mechanisms of human uterine contractility in physiological and pathological contexts. This knowledge will likely reveal opportunities for new therapies to address any number of conditions associated with abnormal uterine contractility. Furthermore, these systems can also serve as testbeds for evaluating the safety and efficacy of drugs and other small molecules on uterine function.

LIMITATIONS OF THE STUDY

A major limitation of our approach is that cells are in a 2-dimensional format and thus lack many of the complex cell–cell and

cell–matrix interactions that are present in native myometrium or 3-dimensional tissue models. We selected polyacrylamide hydrogels because they enable the deformability required to measure force generation and better mimic the rigidity of soft tissues. While the elastic modulus of our hydrogel is slightly lower than what may be found in native myometrium,⁹⁴ it is within the same order of magnitude and is soft enough to exhibit measurable deformation caused by these cells. Another limitation is the use of purified fibronectin, which does not represent the diversity of native myometrial ECM.⁹⁵ Future modifications to the platform may incorporate additional matrix proteins, such as collagen, elastin, or proteoglycans. Our model also lacks physiological cell–cell interactions, as the tissues comprise purified myometrial smooth muscle cells without any vasculature or immune cells.⁸¹ These supporting cells likely play a key role in regulating myometrial contractility. We also used primary cells isolated from only one patient, and thus our data may not be representative of the general population. We are also unaware of the pregnancy state of the patient or the region of origin of the cells within the uterus, which are critical variables that can be investigated in future studies. The concentrations of our small molecules are also vastly higher than *in vivo* measurements, likely due to a loss of sensitivity caused by *in vitro* culture.

METHODS

Fabrication of PDMS stamps

A chrome photomask with $200 \times 100 \mu\text{m}^2$ rectangular voids separated by a minimum of $500 \mu\text{m}$ was designed in AutoCAD (AutoDesk) and manufactured by the UCLA Nanolab mask shop. The photomask was positioned in a mask aligner (Suss MicroTec) above a silicon wafer spin-coated with SU-8 2005 negative photoresist (MicroChem Corp), which was then exposed to UV light based on manufacturer recommendations. The exposed photoresist was then developed, resulting in wafers with raised rectangular features. Sylgard 184 polydimethylsiloxane (PDMS) (Dow Corning) was cast and cured on the master molds to create template stamps with rectangular voids. PDMS was also cast and cured onto featureless wafers to create flat stamps.

Fabrication of polyacrylamide hydrogels

Similar to previous studies,^{41,96} 25 mm glass coverslips were submerged in sodium hydroxide (0.1 M) for 5 min, (3-Aminopropyl)triethoxysilane (APTES) (0.5% v/v in 95% ethanol) for 5 min, fresh 95% ethanol 3 times for 5 min each, and glutaraldehyde (0.5% v/v in ultrapure water) for 30 min, then rinsed with water. Polyacrylamide hydrogels were prepared as previously described.⁹⁶ Briefly, 40% acrylamide (Bio-Rad), 2% N,N'-methylenebisacrylamide (Sigma-Aldrich), and ultrapure water were combined in a ratio of 5:2:5.⁴¹ $9 \mu\text{l}$ of TEMED (Thermo Fisher Scientific) was added to 2.501 ml water. $180 \mu\text{l}$ of the acrylamide mixture was combined with $60 \mu\text{l}$ of $10 \times$ PBS, $6 \mu\text{l}$ of fluorescent microparticles (Invitrogen, $0.2 \mu\text{m}$, yellow-green 505/515), $251 \mu\text{l}$ of the TEMED solution, and $3 \mu\text{l}$ of 10% ammonium persulfate. $50 \mu\text{l}$ of this solution was supplemented with $10 \mu\text{l}$ streptavidin acrylamide (Invitrogen). $20 \mu\text{l}$ of the final solution was pipetted onto an activated 25 mm coverslip, flattened with a non-activated 18 mm coverslip, then left undisturbed for 45 min for polymerization. Once fully cured, the non-activated coverslip was removed from the hydrogel using a razor blade and the remaining glass coverslip with hydrogel was rinsed and submerged in PBS for storage at 4°C .

Microcontact printing

Lyophilized fibronectin (Corning) was incubated with aqueous sodium carbonate and sulfo-NHS-LC-biotin (ThermoFisher) overnight, then dialyzed to remove unconjugated biotin. The remaining biotinylated fibronectin was collected and stored at 4°C . To microcontact print the hydrogel, flat PDMS stamps were incubated with diluted biotinylated fibronectin ($200 \mu\text{g}/\text{ml}$ in PBS) for an hour, then dried with compressed air. Similar to previous studies,⁹⁷ template stamps with rectangular voids were placed in a UVO Cleaner model 342 (Jelight Company) for 20 min then pressed against fibronectin-coated flat stamps. The template stamp was then removed and the flat stamp was pressed onto dried polyacrylamide hydrogels. The substrate was rinsed then submerged in PBS, exposed to low levels of UV light in a biosafety cabinet for sterilization, and stored at 4°C until cell seeding.

Myometrial smooth muscle cell culture

Cell culture media was prepared by combining vascular cell basal medium (ATCC PCS-100-030), vascular smooth muscle cell growth kit (ATCC PCS-100-042), including fetal bovine serum, and penicillin–streptomycin (0.1%) and sterilizing with a $0.22 \mu\text{m}$ vacuum filter. Human myometrial smooth muscle cells (ATCC) were obtained at passage two, expanded, cryopreserved, and thawed as needed for experiments at passage four. T75 tissue culture flasks were incubated with 0.1% gelatin (Stem Cell Technologies) for 30 min, followed by incubation with cell culture media for 30 min. A cryopreserved cell aliquot was then thawed for 2 min at 37°C , resuspended in 3 ml media, and divided amongst four T75 flasks. Cells attached for a minimum of one day, then were detached using 0.5% trypsin-EDTA and seeded onto prepared coverslips at a density of 150 000 cells per 3 ml media in a 6-well plate. After 24–36 h, cells were observed for attachment to the micropatterned fibronectin rectangles, then serum starved for 12 h prior to live imaging.

Immunostaining and characterization of tissue structure

For immunostaining, cells were cultured on hydrogel substrates prepared without fluorescent beads. Seeded coverslips were fixed by rinsing with PBS, incubating for 10 min with 4% paraformaldehyde and 0.2% TritonX-100, then rinsing again in PBS prior to storing for up to one week at 4°C . To stain, coverslips were incubated for 1.5 h with rabbit anti-fibronectin antibody (Sigma Aldrich, 1:200), rinsed three times in PBS, then incubated again for 1.5 h with DAPI (Invitrogen, 1:200), Phalloidin (Life Technologies, 1:200), and Alexa Fluor 546 goat anti-rabbit antibody (Invitrogen 1:200). Coverslips were again rinsed three times in PBS before mounting on microscope glass slides with prolong Gold antifade (Invitrogen) and sealed with nail polish.

Stained coverslips were imaged using a $20 \times$ objective on a Nikon Ti inverted fluorescence microscope with Andor Zyla scientific CMOS camera. Nuclei per island were counted using DAPI signal and ImageJ Analyze Particles. Island size was calculated using fibronectin signal and ImageJ. Cytoskeletal alignment was calculated using actin signal and ImageJ OrientationJ. Data are displayed as mean \pm standard error of the mean.

Traction force microscopy

Tissues were serum starved for a minimum of 12 h before imaging. 15 min before imaging, coverslips were rinsed three times with Tyrode's solution (5.0 mM HEPES, 1.0 mM magnesium chloride, 5.4 mM potassium chloride, 135.0 mM sodium chloride, 0.33 mM potassium phosphate, 1.8 mM calcium chloride, 5.0 mM D-glucose, and pH 7.4 at 37 °C), then transferred in 300 μ l Tyrode's solution to a temperature-controlled imaging chamber mounted on a Nikon Ti inverted fluorescence microscope with Andor Zyla scientific CMOS camera. Movement of fluorescent beads was captured using the 10 \times objective, 1.5 \times zoom, at a frame rate of one image per minute for 12 min. Trypsin-EDTA (0.05%) was then added at a ratio of 1:1 for the purpose of identifying the original or force-free location of fluorescent beads, and images were collected for an additional 6 min. The treatment durations were decided empirically. Brightfield images of tissues were taken before the contraction, before the addition of trypsin, and after the trypsin exposure.

To measure response to oxytocin, one fluorescent bead image was captured before the addition of 300 μ l phosphate buffered saline (PBS) or 300 μ l synthetic oxytocin (1 mM) (Sigma Aldrich) in PBS for a final concentration of 0.5 mM. For drug response experiments, cells were pre-incubated with progesterone or caffeine prior to imaging, then 1 mM of oxytocin was added after the first bead image was captured. Progesterone (Millipore Sigma, 0.127 mM) was added to serum-free media and incubated for a minimum of 12 h before imaging. Caffeine (Sigma Aldrich) was combined with Tyrode's for a concentration of 10.3 mM and added to coverslips during adjustment time on the microscope for a total of 10 min of incubation. To measure responses to inflammatory mediators, 300 μ l of prostaglandins [2 μ M for prostaglandin E1 (PGE1), prostaglandin E2 (PGE2), and prostaglandin F2 α (PGF), Sigma Aldrich]⁹⁸ or cytokines [2 μ g/ml in PBS for interleukin-6 (IL-6) and interleukin-8 (IL-8), R&D systems]^{32,99} were added immediately after the first reference image was collected.

Matlab was used to quantify bead displacement and force generation, as previously described.^{41,100} Briefly, an image sequence of the beads from a given tissue was uploaded. Each frame was divided into a grid with 4096 squares, each 6.88 \times 6.88 μ m². Each element of each frame was compared to the corresponding element in the initial frame to develop a displacement vector field. The three maximum vectors of each frame were averaged, then all tissues within one condition were averaged to develop a displacement vs time graph. A second order polynomial equation was fit to the displacement curves and the second coefficient (B1) of the equation was compared for each curve. For induced force responses, the frame used to calculate the peak of the contraction or relaxation was visually selected. The frame used to calculate the basal (unstimulated) force response was consistently identified as the last frame of the trypsin incubation. Using Fourier transform traction cytometry on the displacement vector field, traction stress vectors at the peak of contraction, relaxation, or detachment were calculated. These traction stress vectors were multiplied by their x-coordinate, summed, and then divided by the length of the tissue to calculate either basal or induced force.⁴¹

SUPPLEMENTARY MATERIAL

See the [supplementary material](#) for Video S1, contractile response to oxytocin, related to Fig. 2. (A) Static brightfield image of μ myometrium indicating tissue outline. (B) As μ myometrium

contracts in response to oxytocin, underlying beads displace toward the center of the tissue. (C) Displacement and (D) traction stress heat maps are calculated from bead displacement.

ACKNOWLEDGMENTS

This work was supported by the USC Annenberg Fellowship; USC Graduate School Fellowship (A.P.M.); NSF CAREER Award No. CMMI 1944734 (M.L.M.); NSF GRFP Award No. DGE-1842487 (A.P.M.); the Center for Undergraduate Research in Viterbi Engineering (CURVE) Fellowships (J.M.T., S.J.W.); and the USC Viterbi School of Engineering. We acknowledge the USC Nanofabrication Core for photolithography equipment and facilities. We thank Dr. Brendan Grubbs for helpful discussion about current clinical trends.

AUTHOR DECLARATIONS

Conflict of Interest

The authors have no conflicts to disclose.

Ethics Approval

Ethics approval is not required.

Author Contributions

Antonina P. Maxey: Conceptualization (equal); Formal analysis (lead); Investigation (lead); Methodology (equal); Software (lead); Visualization (equal); Writing – original draft (equal); Writing – review & editing (equal). **Sage J. Wheeler:** Formal analysis (supporting); Investigation (supporting). **Jaya M. Travis:** Investigation (supporting). **Megan L. McCain:** Conceptualization (lead); Funding acquisition (lead); Methodology (equal); Resources (lead); Supervision (lead); Visualization (equal); Writing – original draft (equal); Writing – review & editing (equal).

Data AVAILABILITY

The data that support the findings of this study are available from the corresponding author upon reasonable request.

REFERENCES

- ¹H. A. Frey and M. A. Klebanoff, "The epidemiology, etiology, and costs of preterm birth," *Semin. Fetal Neonatal Med.* **21**(2), 68–73 (2016).
- ²E. R. Norwitz and A. B. Caughey, "Progesterone supplementation and the prevention of preterm birth," *Rev. Obstet. Gynecol.* **4**(2), 60–72 (2011).
- ³R. L. Goldenberg, "The management of preterm labor," *Obstet. Gynecol.* **100**(5 Pt 1), 1020–1037 (2002).
- ⁴A. López Bernal, "Overview. Preterm labour: Mechanisms and management," *BMC Pregnancy Childbirth* **7**(Suppl 1), S2 (2007).
- ⁵B. Pehlivanoglu, S. Bayrak, and M. Dogan, "A close look at the contraction and relaxation of the myometrium; the role of calcium," *J. Turkish German Gynecol. Assoc.* **14**, 230 (2013).
- ⁶Z. Barcikowska *et al.*, "Inflammatory markers in dysmenorrhea and therapeutic options," *Int. J. Environ. Res. Public Health* **17**(4), 1191 (2020).
- ⁷R. Itani *et al.*, "Primary dysmenorrhea: Pathophysiology, diagnosis, and treatment updates," *Korean J. Fam. Med.* **43**(2), 101–108 (2022).
- ⁸S. T. Wu *et al.*, "Maternal risk factors for preterm birth in Taiwan, a nationwide population-based cohort study," *Pediatr. Neonatol.* **65**, 38 (2024).

- ⁹T. Murata *et al.*, "Association of preconception dysmenorrhea with obstetric complications: The Japan Environment and Children's Study," *BMC Pregnancy Childbirth* **22**(1), 125 (2022).
- ¹⁰M. Hadzi Lega *et al.*, "Interleukin 6 and fetal fibronectin as predictors of preterm delivery in symptomatic patients," *Biomol. Biomed.* **15**(1), 51–56 (2015).
- ¹¹H. Ma *et al.*, "Altered cytokine gene expression in peripheral blood monocytes across the menstrual cycle in primary dysmenorrhea: A case-control study," *PLoS One* **8**(2), e55200 (2013).
- ¹²A. Lethaby, K. Duckitt, and C. Farquhar, "Non-steroidal anti-inflammatory drugs for heavy menstrual bleeding," *Cochrane Database Syst. Rev.* **2013**(1), CD000400.
- ¹³R. J. Phillips, M. A. Fortier, and A. López Bernal, "Prostaglandin pathway gene expression in human placenta, amnion and choriondecidua is differentially affected by preterm and term labour and by uterine inflammation," *BMC Pregnancy Childbirth* **14**, 241 (2014).
- ¹⁴M. S. Vidal *et al.*, "Spontaneous preterm birth: Involvement of multiple fetomaternal tissues and organ systems, differing mechanisms, and pathways," *Front. Endocrinol.* **13**, 1015622 (2022).
- ¹⁵M. Ivanisević, J. Djelms, and D. Buković, "Review on prostaglandin and oxytocin activity in preterm labor," *Coll. Antropol.* **25**(2), 687–694 (2001).
- ¹⁶V. Lundström and K. Gréen, "Endogenous levels of prostaglandin F2alpha and its main metabolites in plasma and endometrium of normal and dysmenorrhoeic women," *Am. J. Obstet. Gynecol.* **130**(6), 640–646 (1978).
- ¹⁷J. Marjoribanks *et al.*, "Nonsteroidal anti-inflammatory drugs for dysmenorrhoea," *Cochrane Database Syst. Rev.* **2015**(7), CD001751.
- ¹⁸M. Pandey, M. Chauhan, and S. Awasthi, "Interplay of cytokines in preterm birth," *Indian J. Med. Res.* **146**(3), 316–327 (2017).
- ¹⁹N. M. Orsi and R. M. Tribe, "Cytokine networks and the regulation of uterine function in pregnancy and parturition," *J. Neuroendocrinol.* **20**(4), 462–469 (2008).
- ²⁰M. L. Yeh *et al.*, "A study of serum malondialdehyde and interleukin-6 levels in young women with dysmenorrhea in Taiwan," *Life Sci.* **75**(6), 669–673 (2004).
- ²¹K. Pantos *et al.*, "The role of interleukins in recurrent implantation failure: A comprehensive review of the literature," *Int. J. Mol. Sci.* **23**(4), 2198 (2022).
- ²²A. Arici, "Local cytokines in endometrial tissue: The role of interleukin-8 in the pathogenesis of endometriosis," *Ann. N. Y. Acad. Sci.* **955**, 101 (2002); discussion 118, 396–406.
- ²³T. Shea-Donohue *et al.*, "Mechanisms of smooth muscle responses to inflammation," *Neurogastroenterol. Motil.* **24**(9), 802–811 (2012).
- ²⁴Y. Chiba *et al.*, "Interleukin-13 augments bronchial smooth muscle contractility with an up-regulation of RhoA protein," *Am. J. Respir. Cell Mol. Biol.* **40**(2), 159–167 (2009).
- ²⁵A. P. Nesmith *et al.*, "Human airway musculature on a chip: An *in vitro* model of allergic asthmatic bronchoconstriction and bronchodilation," *Lab Chip* **14**(20), 3925–3936 (2014).
- ²⁶P. H. Abrams and R. C. Feneley, "The actions of prostaglandins on the smooth muscle of the human urinary tract *in vitro*," *Br. J. Urol.* **47**(7), 909–915 (1975).
- ²⁷S. P. Williams, G. W. Dorn, and R. M. Rapoport, "Prostaglandin I2 mediates contraction and relaxation of vascular smooth muscle," *Am. J. Physiol.* **267**(2 Pt 2), H796–803 (1994).
- ²⁸D. M. Slater *et al.*, "Anti-inflammatory and relaxatory effects of prostaglandin E2 in myometrial smooth muscle," *Mol. Hum. Reprod.* **12**(2), 89–97 (2006).
- ²⁹G. Chiossi *et al.*, "The effects of prostaglandin E1 and prostaglandin E2 on *in vitro* myometrial contractility and uterine structure," *Am. J. Perinatol.* **29**(8), 615–622 (2012).
- ³⁰S. Arulkumaran *et al.*, "The roles of prostaglandin EP 1 and 3 receptors in the control of human myometrial contractility," *J. Clin. Endocrinol. Metab.* **97**(2), 489–498 (2012).
- ³¹S. Khatun *et al.*, "Interleukin-8 potentiates the effect of interleukin-1-induced uterine contractions," *Hum. Reprod.* **14**(2), 560–565 (1999).
- ³²U. Friebe-Hoffmann, J. P. Chiao, and P. N. Rauk, "Effect of IL-1beta and IL-6 on oxytocin secretion in human uterine smooth muscle cells," *Am. J. Rep. Immunol.* **46**(3), 226–231 (2001).
- ³³A. P. Maxey and M. L. McCain, "Tools, techniques, and future opportunities for characterizing the mechanobiology of uterine myometrium," *Exp. Biol. Med.* **246**(9), 1025–1035 (2021).
- ³⁴S. Arrowsmith *et al.*, "Contractility Measurements of human uterine smooth muscle to aid drug development," *J. Visualized Exp.* (131), 56639 (2018).
- ³⁵B. W. Nielsen *et al.*, "A cross-species analysis of animal models for the investigation of preterm birth mechanisms," *Reprod. Sci.* **23**(4), 482–491 (2016).
- ³⁶N. Gavara *et al.*, "Thrombin-induced contraction in alveolar epithelial cells probed by traction microscopy," *J. Appl. Physiol.* **101**(2), 512–520 (2006).
- ³⁷B. Hissa *et al.*, "Cholesterol depletion impairs contractile machinery in neonatal rat cardiomyocytes," *Sci. Rep.* **7**, 43764 (2017).
- ³⁸I. M. Tolić-Nørrelykke *et al.*, "Spatial and temporal traction response in human airway smooth muscle cells," *Am. J. Physiol. Cell Physiol.* **283**(4), C1254–66 (2002).
- ³⁹A. Zanca *et al.*, "A primer to traction force microscopy," *J. Biol. Chem.* **298**(5), 101867 (2022).
- ⁴⁰F. S. Pasqualini *et al.*, "Traction force microscopy of engineered cardiac tissues," *PLoS One* **13**(3), e0194706 (2018).
- ⁴¹M. L. McCain *et al.*, "Cooperative coupling of cell-matrix and cell-cell adhesions in cardiac muscle," *Proc. Natl. Acad. Sci. U. S. A.* **109**(25), 9881–9886 (2012).
- ⁴²A. J. S. Ribeiro *et al.*, "Multi-imaging method to assay the contractile mechanical output of micropatterned human iPSC-derived cardiac myocytes," *Circ. Res.* **120**(10), 1572–1583 (2017).
- ⁴³N. R. Ariyasinghe *et al.*, "Engineering micromyocardium to delineate cellular and extracellular regulation of myocardial tissue contractility," *Integr. Biol.* **9**(9), 730–741 (2017).
- ⁴⁴S. Wray and C. Prendergast, "The myometrium: From excitation to contractions and labour," *Adv. Exp. Med. Biol.* **1124**, 233–263 (2019).
- ⁴⁵J. G. Smith and D. C. Merrill, "Oxytocin for induction of labor," *Clin. Obstet. Gynecol.* **49**(3), 594–608 (2006).
- ⁴⁶J. Guo *et al.*, "Elastomer-grafted iPSC-derived micro heart muscles to investigate effects of mechanical loading on physiology," *ACS Biomater. Sci. Eng.* **7**(7), 2973–2989 (2021).
- ⁴⁷M. S. Soloff *et al.*, "Effects of progesterone treatment on expression of genes involved in uterine quiescence," *Reprod. Sci.* **18**(8), 781–797 (2011).
- ⁴⁸M. Lucovnik *et al.*, "Progestin treatment for the prevention of preterm birth," *Acta Obstet. Gynecol. Scand.* **90**(10), 1057–1069 (2011).
- ⁴⁹T. Tazzeo *et al.*, "Caffeine relaxes smooth muscle through actin depolymerization," *Am. J. Physiol. Lung Cell Mol. Physiol.* **303**(4), L334–42 (2012).
- ⁵⁰P. N. Mehta *et al.*, "Dissociation between the effects of theophylline and caffeine on premature airway smooth muscles," *Pediatr. Res.* **29**(5), 446–448 (1991).
- ⁵¹A. P. Maxey, J. M. Travis, and M. L. McCain, "Regulation of oxytocin-induced calcium transients and gene expression in engineered myometrial tissues by tissue architecture and matrix rigidity," *Curr. Res. Physiol.* **6**, 100108 (2023).
- ⁵²X. Chen *et al.*, "Phenylephrine, a common cold remedy active ingredient, suppresses uterine contractions through cAMP signalling," *Sci. Rep.* **8**(1), 11666 (2018).
- ⁵³J. P. Savineau and J. Mironneau, "Caffeine acting on pregnant rat myometrium: Analysis of its relaxant action and its failure to release Ca²⁺ from intracellular stores," *Br. J. Pharmacol.* **99**(2), 261–266 (1990).
- ⁵⁴D. M. Olson and C. Ammann, "Role of the prostaglandins in labour and prostaglandin receptor inhibitors in the prevention of preterm labour," *Front. Biosci.* **12**, 1329–1343 (2007).
- ⁵⁵T. Nagaria and N. Sirmor, "Misoprostol vs mifepristone and misoprostol in second trimester termination of pregnancy," *J. Obstet. Gynecol. India* **61**(6), 659–662 (2011).
- ⁵⁶J. Cao *et al.*, "Uterine region-dependent differences in responsiveness to prostaglandins in the non-pregnant porcine myometrium," *Prostaglandins Other Lipid Mediators* **75**(1–4), 105–122 (2005).
- ⁵⁷N. Dajani, E. Idriss, and P. L. Collins, "Interleukin-6 does not stimulate rat myometrial contractions in an *in vitro* model," *Am. J. Rep. Immunol.* **32**(3), 248–254 (1994).
- ⁵⁸K. Uvnäs-Moberg, "The physiology and pharmacology of oxytocin in labor and in the peripartum period," *Am. J. Obstet. Gynecol.* **230**(3S), S740–S758 (2024).
- ⁵⁹K. Uvnäs-Moberg *et al.*, "Maternal plasma levels of oxytocin during physiological childbirth—A systematic review with implications for uterine contractions and central actions of oxytocin," *BMC Pregnancy Childbirth* **19**(1), 285 (2019).

- ⁶⁰A. R. Fuchs *et al.*, "Oxytocin secretion and human parturition: Pulse frequency and duration increase during spontaneous labor in women," *Am. J. Obstet. Gynecol.* **165**(5 Pt 1), 1515–1523 (1991).
- ⁶¹R. Chibbar, F. D. Miller, and B. F. Mitchell, "Synthesis of oxytocin in amnion, chorion, and decidua may influence the timing of human parturition," *J. Clin. Invest.* **91**(1), 185–192 (1993).
- ⁶²T. Kimura *et al.*, "Expression of oxytocin receptor in human pregnant myometrium," *Endocrinology* **137**(2), 780–785 (1996).
- ⁶³A. Shmygol *et al.*, "Multiple mechanisms involved in oxytocin-induced modulation of myometrial contractility," *Acta Pharmacol. Sin.* **27**(7), 827–832 (2006).
- ⁶⁴R. C. Tuckey, "Progesterone synthesis by the human placenta," *Placenta* **26**(4), 273–281 (2005).
- ⁶⁵G. Gimpl and F. Fahrenholz, "The oxytocin receptor system: Structure, function, and regulation," *Physiol. Rev.* **81**(2), 629–683 (2001).
- ⁶⁶J. D. Younger, E. Reitman, and G. Gallos, "Tocolysis: Present and future treatment options," *Semin. Perinatol.* **41**(8), 493–504 (2017).
- ⁶⁷J. Verhaegen *et al.*, "Accuracy of single progesterone test to predict early pregnancy outcome in women with pain or bleeding: Meta-analysis of cohort studies," *BMJ* **345**, e6077 (2012).
- ⁶⁸M. Duport Percier *et al.*, "Serum progesterone concentration on pregnancy test day might predict ongoing pregnancy after controlled ovarian stimulation and fresh embryo transfer," *Front. Endocrinol.* **14**, 1191648 (2023).
- ⁶⁹H. Okubo *et al.*, "Maternal total caffeine intake, mainly from Japanese and Chinese tea, during pregnancy was associated with risk of preterm birth: The Osaka Maternal and Child Health Study," *Nutr. Res.* **35**(4), 309–316 (2015).
- ⁷⁰D. Modzelewska *et al.*, "Caffeine exposure during pregnancy, small for gestational age birth and neonatal outcome—Results from the Norwegian Mother and Child Cohort Study," *BMC Pregnancy Childbirth* **19**(1), 80 (2019).
- ⁷¹W. Gibb, "The role of prostaglandins in human parturition," *Ann. Med.* **30**(3), 235–241 (1998).
- ⁷²E. Ricciotti and G. A. FitzGerald, "Prostaglandins and inflammation," *Arterioscler., Thromb., Vasc. Biol.* **31**(5), 986–1000 (2011).
- ⁷³L. Myatt and S. J. Lye, "Expression, localization and function of prostaglandin receptors in myometrium," *Prostaglandins, Leukotrienes Essent. Fatty Acids* **70**(2), 137–148 (2004).
- ⁷⁴Y. C. Ruan, W. Zhou, and H. C. Chan, "Regulation of smooth muscle contraction by the epithelium: Role of prostaglandins," *Physiology* **26**(3), 156–170 (2011).
- ⁷⁵M. Patwardhan *et al.*, "Dynamic changes in the myometrium during the third stage of labor, evaluated using two-dimensional ultrasound, in women with normal and abnormal third stage of labor and in women with obstetric complications," *Gynecol. Obstet. Invest.* **80**(1), 26–37 (2015).
- ⁷⁶R. E. Garris and C. F. Kirkwood, "Misoprostol: A prostaglandin E1 analogue," *Clin. Pharm.* **8**(9), 627–644 (1989).
- ⁷⁷G. Chiosso *et al.*, "In vitro myometrial contractility profiles of different pharmacological agents used for induction of labor," *Am. J. Perinatol.* **29**(9), 699–704 (2012).
- ⁷⁸G. C. Smith *et al.*, "Regional variations in contractile responses to prostaglandins and prostanoid receptor messenger ribonucleic acid in pregnant baboon uterus," *Am. J. Obstet. Gynecol.* **179**(6 Pt 1), 1545–1552 (1998).
- ⁷⁹D. M. Paternoster *et al.*, "Biochemical markers for the prediction of spontaneous pre-term birth," *Int. J. Gynecol. Obstet.* **79**(2), 123–129 (2002).
- ⁸⁰A. Sebba, "Tocilizumab: The first interleukin-6-receptor inhibitor," *Am. J. Health Syst. Pharm.* **65**(15), 1413–1418 (2008).
- ⁸¹K. Ji *et al.*, "Integrating single-cell RNA sequencing with spatial transcriptomics reveals an immune landscape of human myometrium during labour," *Clin. Transl. Med.* **13**(4), e1234 (2023).
- ⁸²S. Landau *et al.*, "Primitive macrophages enable long-term vascularization of human heart-on-a-chip platforms," *Cell Stem Cell* **31**(8), 1222–1238 e10 (2024).
- ⁸³G. R. Souza *et al.*, "Magnetically bioprinted human myometrial 3D cell rings as a model for uterine contractility," *Int. J. Mol. Sci.* **18**(4), 683 (2017).
- ⁸⁴L. Madden *et al.*, "Bioengineered human myobundles mimic clinical responses of skeletal muscle to drugs," *Elife* **4**, e04885 (2015).
- ⁸⁵K. Ronaldson-Bouchard *et al.*, "Advanced maturation of human cardiac tissue grown from pluripotent stem cells," *Nature* **556**(7700), 239–243 (2018).
- ⁸⁶E. Dimitriadis *et al.*, "Cytokines, chemokines and growth factors in endometrium related to implantation," *Hum. Reprod. Update* **11**(6), 613–630 (2005).
- ⁸⁷R. Raghupathy, "Cytokines as key players in the pathophysiology of pre-eclampsia," *Med. Princ. Pract.* **22**(Suppl 1), 8–19 (2013).
- ⁸⁸M. Hoang *et al.*, "Human fetal membranes generate distinct cytokine profiles in response to bacterial Toll-like receptor and nod-like receptor agonists," *Biol. Reprod.* **90**(2), 39 (2014).
- ⁸⁹T. H. C. De Bem *et al.*, "Endometrium on-a-chip reveals insulin- and glucose-induced alterations in the transcriptome and proteomic secretome," *Endocrinology* **162**(6), bqab054 (2021).
- ⁹⁰J. Ahn *et al.*, "Three-dimensional microengineered vascularised endometrium-on-a-chip," *Hum. Reprod.* **36**(10), 2720–2731 (2021).
- ⁹¹A. Lermant *et al.*, "Development of a human iPSC-derived placental barrier-on-chip model," *iScience* **26**(7), 107240 (2023).
- ⁹²J. S. Lee *et al.*, "Placenta-on-a-chip: A novel platform to study the biology of the human placenta," *J. Matern.-Fetal Neonat. Med.* **29**(7), 1046–1054 (2016).
- ⁹³S. Xiao *et al.*, "A microfluidic culture model of the human reproductive tract and 28-day menstrual cycle," *Nat. Commun.* **8**, 14584 (2017).
- ⁹⁴R. Rogers *et al.*, "Mechanical homeostasis is altered in uterine leiomyoma," *Am. J. Obstet. Gynecol.* **198**, 474.e1 (2008).
- ⁹⁵P. C. Leppert, F. L. Jayes, and J. H. Segars, "The extracellular matrix contributes to mechanotransduction in uterine fibroids," *Obstet. Gynecol. Int.* **2014**, 783289.
- ⁹⁶M. L. Rexius-Hall, N. R. Ariyasinghe, and M. L. McCain, "Engineering shape-controlled microtissues on compliant hydrogels with tunable rigidity and extracellular matrix ligands," *Methods Mol. Biol.* **2258**, 57–72 (2021).
- ⁹⁷R. A. Desai, N. M. Rodriguez, and C. S. Chen, "Stamp-off" to micropattern sparse, multicomponent features," *Methods Cell Biol.* **119**, 3–16 (2014).
- ⁹⁸A. Mueller *et al.*, "Uterine contractility in response to different prostaglandins: Results from extracorporeally perfused non-pregnant swine uteri," *Hum. Reprod.* **21**(8), 2000–2005 (2006).
- ⁹⁹S. A. Robertson *et al.*, "Interleukin-6 is an essential determinant of on-time parturition in the mouse," *Endocrinology* **151**(8), 3996–4006 (2010).
- ¹⁰⁰P. L. Kuo *et al.*, "Myocyte shape regulates lateral registry of sarcomeres and contractility," *Am. J. Pathol.* **181**(6), 2030–2037 (2012).